Facies analysis and diagenetic evolution of the Dinantian carbonates in the Dutch subsurface: data and analyses well GVK-01

Report by SCAN

October 2019

Ministerie van Economische Zaken en Klimaat
ebn
TNO
Interreg North-West Europe DGE-ROLLOUT

Facies analysis and diagenetic evolution of the Dinantian carbonates in the Dutch subsurface: data and analyses well GVK-01

Written by:
Mahtab Mozafari[1], Peter Gutteridge[2], Alberto Riva[3], Kees Geel[4], Joanna Garland[2] and Julie Dewit[2]

October 2019

1- Energie Beheer Nederland (EBN), Daalsesingel 1, 3511 SV Utrecht, the Netherlands
2- Cambridge Carbonates Ltd, No. 4 The Courtyard, 707 Warwick Road, Solihull, B91 3DA, UK
3- G.E.Plan Consulting srl, Via L. Ariosto 58, 44121 Ferrara, Italy
4- Geological Survey of the Netherlands (TNO), Princetonlaan 6, 3584 CB Utrecht, the Netherlands

Dit rapport is een product van het SCAN-programma en wordt mogelijk gemaakt door het Ministerie van Economische Zaken en Klimaat

Table of contents

3. Geverik 1 (GVK-01)

3.1 Introduction

The GVK-01 well is located in the northern Maastricht area, SE Netherlands (Figures 3-1 and 3-2, Table 3-1). GVK-01 was drilled in 1986 for geological exploration until the depth of 1607 m. The purpose, apparently, was to develop a geothermal plant (OPAC) that was never constructed.

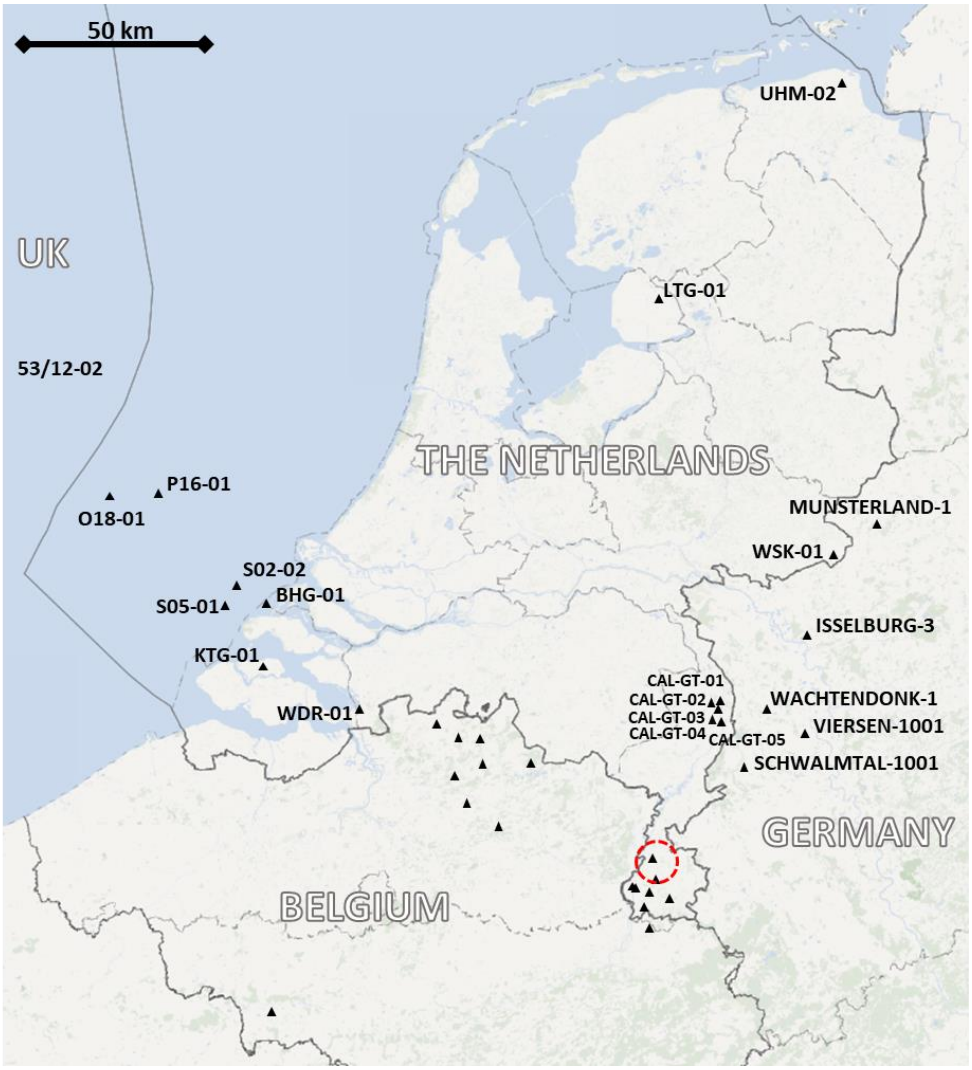

Figure 3-1: Map showing all the wells penetrating the Dinantian carbonates. Location of the GVK-01 well is indicated by a dashed red circle.

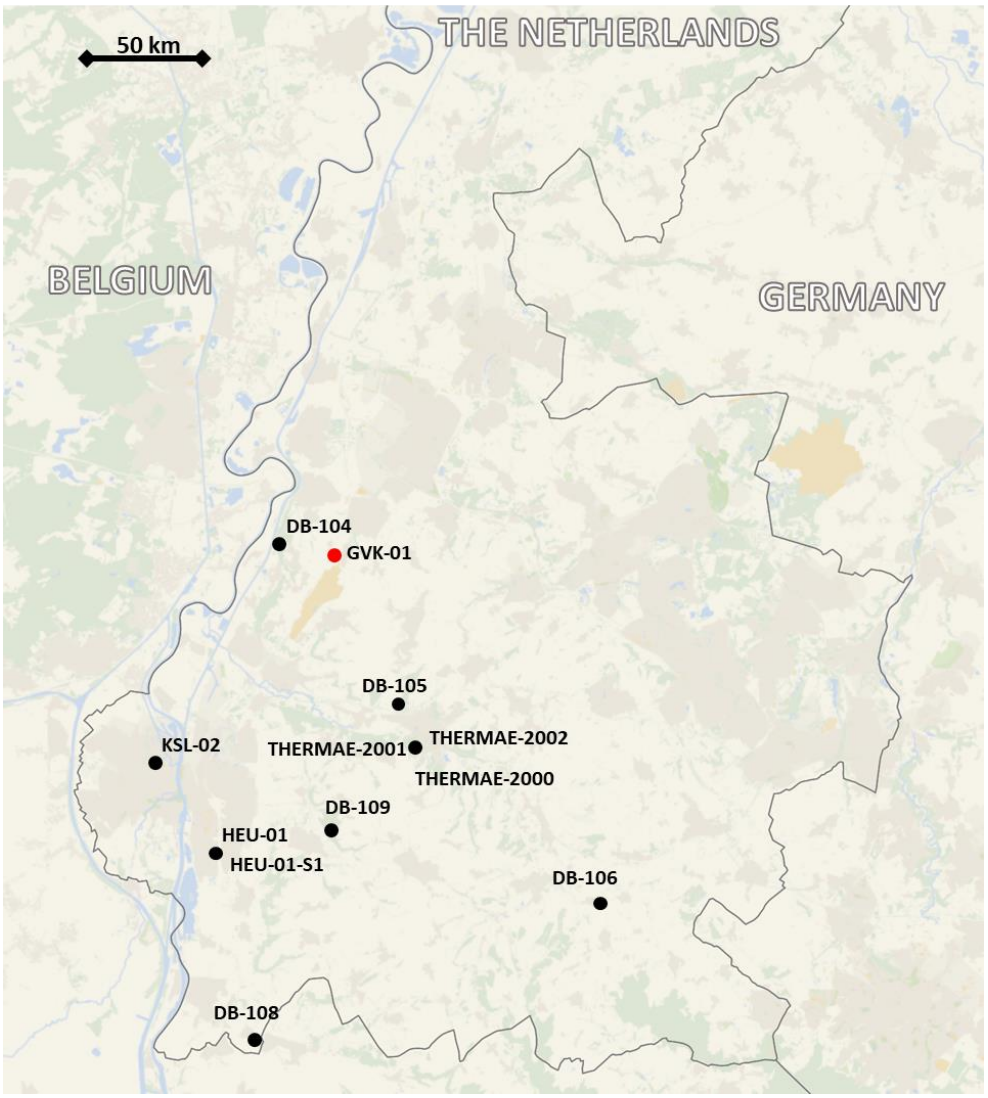

Figure 3-2: Map showing location of the GVK-01 well (red circle).

Table 3-1: Coordinates and depth of GVK-01 well (from www.nlog.nl).

Co-ordinates (x, y in utm31, ed50 format)	695370, 5645498
Lat/Long (°)	50.92695227, 5.77997526
Supplied co-ordinates	182530, 326340 (RD)
Depth in meters referred to:	Rotary Table
Total depth (m, along hole):	1687
Vertical position of Ground Level:	107 meter t.o.v. NAP
Trajectory shape:	Vertical
Deviation in X-direction:	0
Deviation in Y-direction:	0
True vertical depth (TVD) in m:	1687

Table 3-2: Drilling data about GVK-01 well (from www.nlog.nl).

Client name	NEO
Start date	1-May-1986
End date	20-May-1986
Drilling company	Walter GmbH
Type of well	Exploration
Result	Dry
Status	Abandoned

3.2 Available dataset

Some documents, including scanned well logs are present on "www.nlog.nl" within the following link:
https://www.nlog.nl/nlog/requestData/nlogp/allBor/metaData.jsp?tableName=BorLocation&id=106518840
The most relevant publications/reports used in this study are Nyhuis (2012) and Nyhuis et al. (2016). Other relevant publications/reports well are as following:

CoreLab. (2013). Advanced Core Analysis Study, Wintershall, Geverik-1 Well, The Netherlands. Houston.

Dusar, M. (1990). Interpretatie der boorgatmetingen in de boringen Halen (Kb 131) en Geverik -1 (NL Limburg, Gem. Beek), 5 pp.

Elf Aquitaine Production (1996). The Netherlands Onshore; GEVERIK-1 well study, 14 pp.

Fattah, R. A., and Verweij, J. M. (2014). Maturity of carboniferous source rocks in Central Onshore Netherlands. the impact of the Permian thermal anomaly. In First EAGE Basin & Petroleum Systems Modeling Workshop.

Fermont, W. J. J. (1986). Koolpetrografisch onderzoek aan monsters uit het Namurien van de boring Geverik, ten behoeve van het OPAC-project. Heerlen.

Huggett, J. M. (2012). X-ray diffraction semi-quantitative mineralogical analysis of 52 samples from Geverik I. Heathfield.

Laenen, B. (2003). Lithostratigrafie van het pre-Tertiair in Vlaanderen. Deel II: Dinantiaan and Devoon.

Mathes-Schmidt, M. E. (2000). Mikrofazies, Sedimentationsgeschehen und paläogeographische Entwicklung im Verlauf des oberen Viséums im Untergrund der Niederrheinischen Bucht und des Campine-Beckens. Ph.D. thesis, University of Aachen (Germany), 245 pp.

Meesen, J. P. M. T. (1987). Rapport betreffende ltet onderzoek naar mariene microfossielen van twee trajecten uit boring Geverik. Heerlen.

Nyhuis, C. J. (2012). Geverik-01 Thin-Section Report.

Nyhuis, C. J., Riley, D., and Kalasinska, A. (2016). Thin section petrography and chemostratigraphy: Integrated evaluation of an upper Mississippian mudstone dominated succession from the southern Netherlands. Geologie En Mijnbouw/Netherlands Journal of Geosciences, 95, 3-22. https://doi.org/10.1017/njg.2015.25

Van Amerom, H. W. J. (1986). Cumulatief rapport betreffende de stratigrafie van de boring Geverik. Heerlen.

Van Amerom, H. W. J. (1986). Rapport over een voorlopige ouderdomsbepalíno van diepboring Geverik op qrond van plantenfossielen. Heerlen.

Van de Laar, J. G. M. (1987). Resultaten van het voorlopig Micropalaeontologisch/ Palynologisch onderzoek van boring Geverik-1. Report GB2142, Heerlen.

Van Tongeren, P. C. H. (2006). De Vlaamse Voerstreek: een geologische analyse van het Laat Paleozoïcum van deze regio en van het direct aangrenzend gebied (Vol. 2005/MAT/R).

3.2.1 Logs

This well has a complete suite of logs and has been evaluated within the frame of the SCAN project. However, the lower section is incomplete: the gamma ray stops at 1671 m MD and most of the logs usable for the formation evaluation stop at 1508 m.

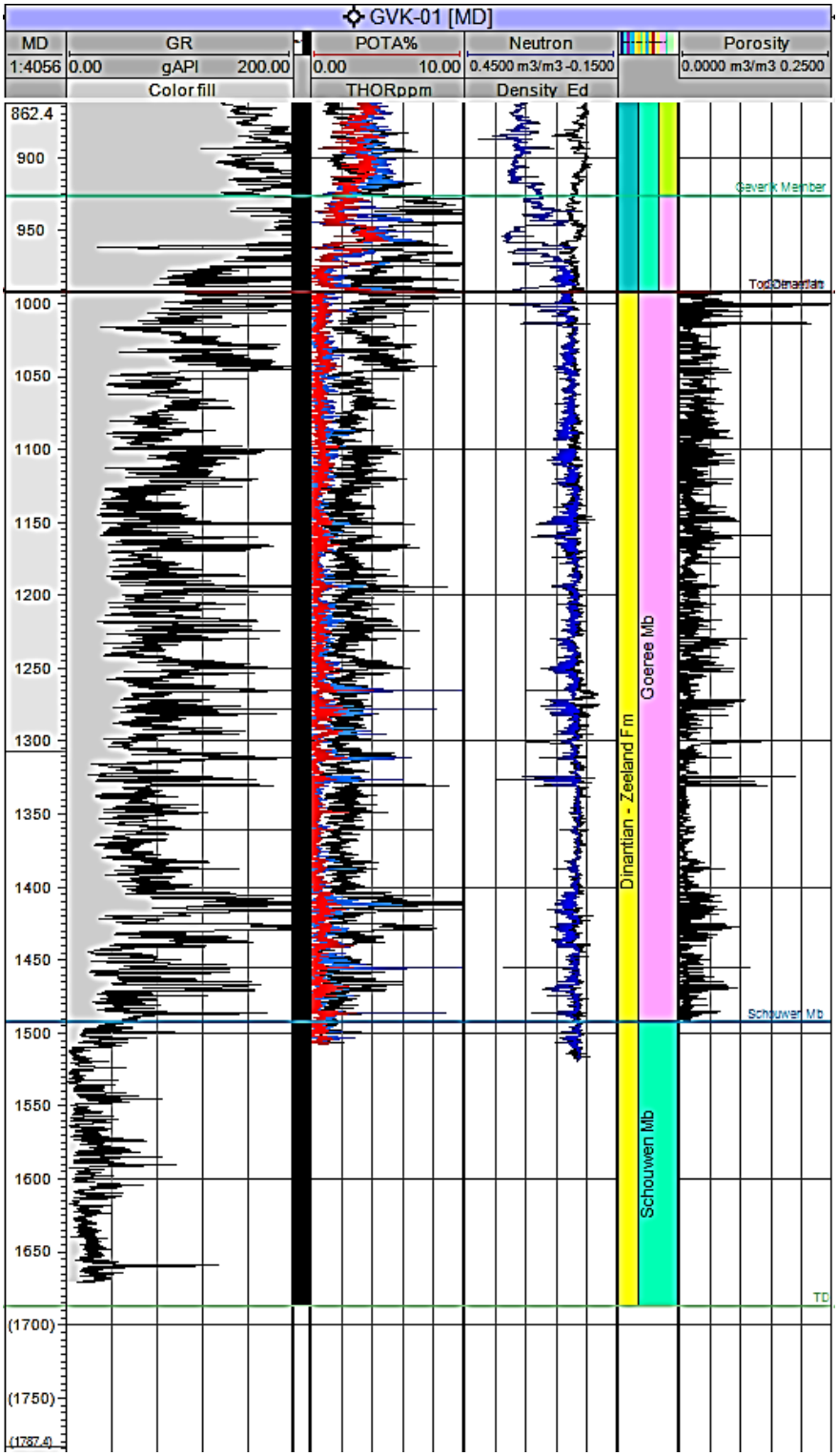

Figure 3.3: Gamma ray, spectral gamma ray components, neutron/density and porosity logs in the GVK-01 well.

3.2.2 Cores, sidewall cores and cuttings

The Dinantian interval was fully cored until TD, with very detailed description by and Mathes-Schmidt (2000) and Nyhuis et al. (2016).

3.2.3 Petrography

A total number of 17 thin sections are present and described by Nyhuis et al. (2016). The latter study showed the predominance of silicified lime mudstone with sponge spicules and abundant comminuted bioclasts (Figure 3-4).

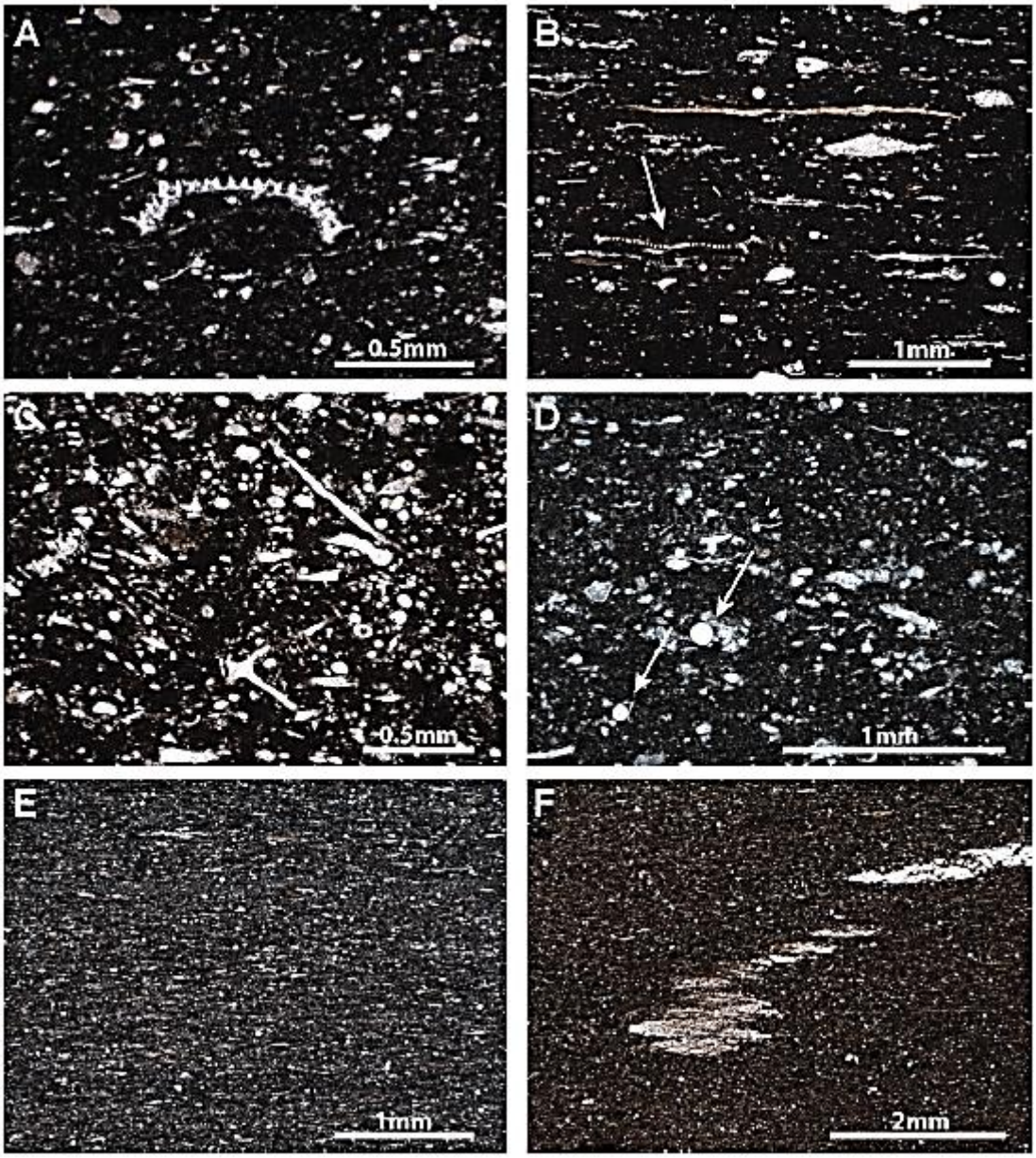

Figure 3-4: A) MFA-1, detailed view of a silicified lime mudstone shows disarticulated entomozoan valve. Note the characteristic spinose shell surface (1045.27 m). B) Calcareous mudstone with abundant flattened bioclasts. Arrow highlights position of entomozoan valve (980.10 m). C) Wackestone with abundant sponge spicules. Note presence of tetraxon and monaxon spicules (975.35 m). D) Another example of a wackestone. It shows two perfectly round radiolarians (arrows) and very fine bioclasts (1.019.20 m). E) This calcareous mudstone shows a relatively strong silicification and a relict lamination (?bioturbation) as well as a lack of larger components (1028.75 m). F) Stacked pattern of silt-filled Planolites burrows within a mudstone. Note homogeneous mudstone fabric (972.75 m) (from Nyhuis et al., 2016).

3.2.4 Fluid inclusions microthermometry

In the Nyhuis (2012) dataset, five samples (four in the Epen Formation, one in the Goeree Member) were analysed for a total of 49 measurements of homogenisation temperature. The obtained T_{ice} values indicate influence of meso- to hypersaline fluids.

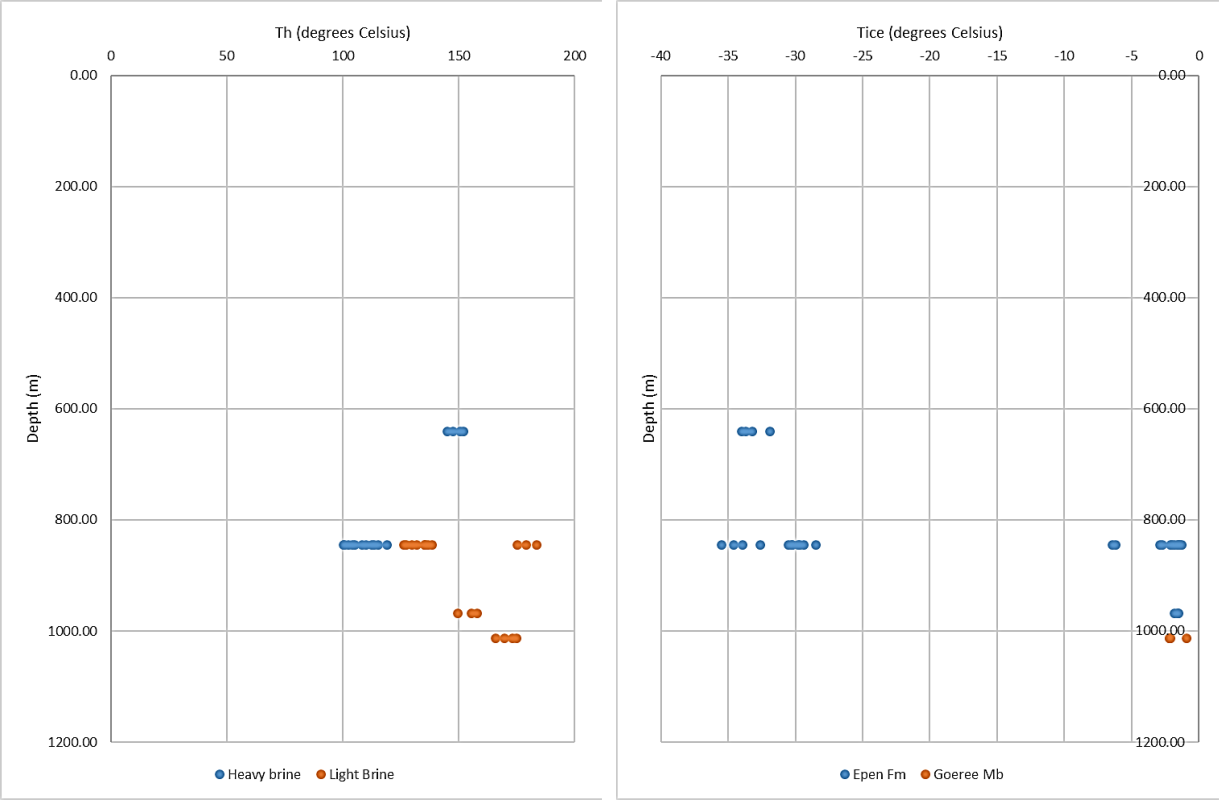

Figure 3-5: Fluid inclusions data modified from the Nyhuis (2012).

3.2.5 Stable carbon and oxygen isotopes

In the Nyhuis (2012) dataset, nine carbon and oxygen isotope analyses performed on the Epen Formation (n = 7) and the Goeree Member of the Zeeland Formation (n = 2) (Figure 3-6). The samples were taken from the cements of several calcite veins. Unfortunately, the isotopic analysis does not correspond with the same samples on which the fluid inclusion microthermometry was performed.

The oxygen isotopes appear quite depleted for both the Namurian and the Dinantian samples and the carbon is depleted as well.

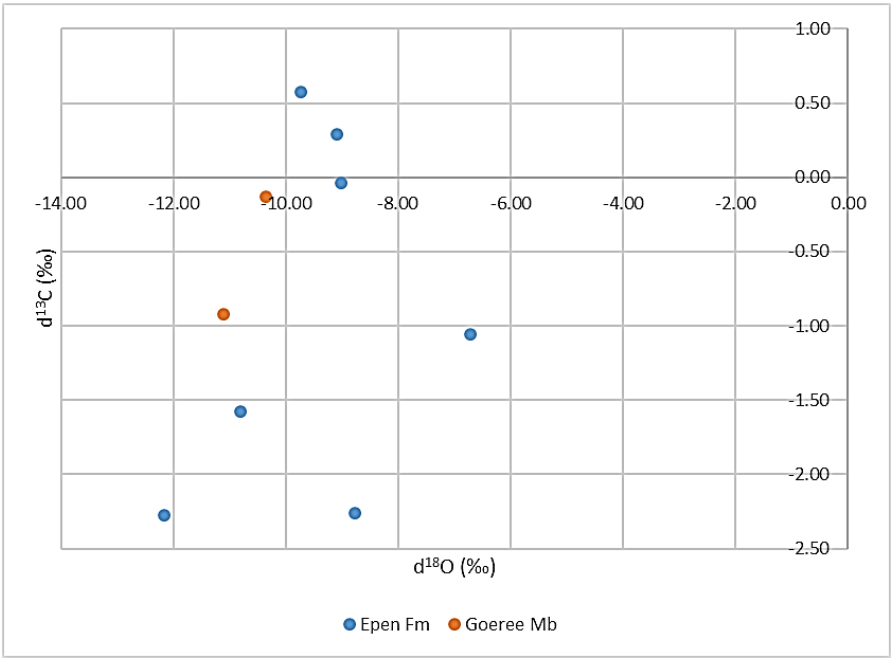

Figure 3-6: Carbon and oxygen isotopic composition of the samples measured from the GVK-01 well (modified after Nyhuis, 2012).

3.2.6 Total Organic Carbon (TOC)

Nyhuis (2012) reported the rock eval analysis (TOC) of a total number of 12 samples from Goeree Member (Figure 3-7). Some of the results appear not to be reliable, as the T_{max} values are very low (<400 °C).

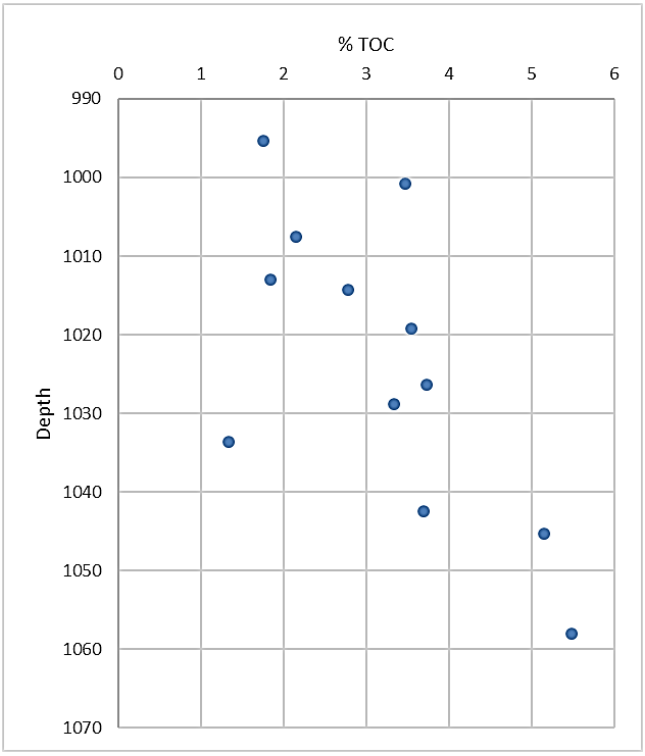

Figure 3-7: TOC values vs depth (m) in the GVK-01 well.

3.2.7 Vitrinite reflectance

Two different sets of vitrinite reflectance data are available for this well, nine measurements from Fermont (1986) and twelve measurements from the Nyhuis (2012). Both datasets are comparable and considered reliable (Figure 3-8).

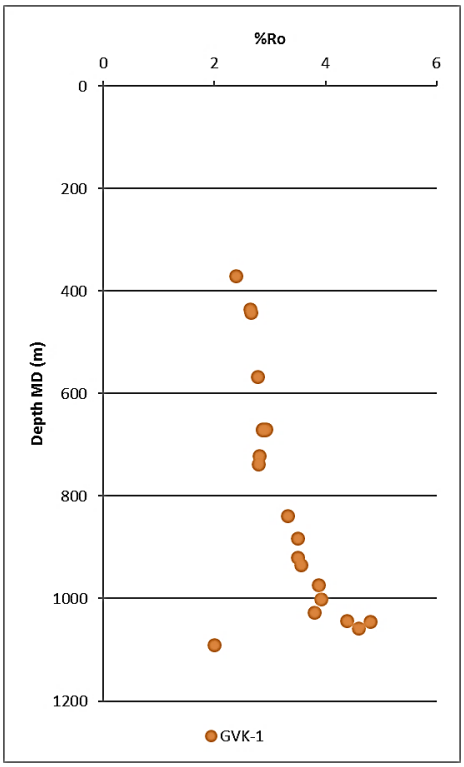

Figure 3-8: Vitrinite reflectance data obtained for the GVK-01 well.

3.3 Stratigraphy

The successions within the Geverik-01 well (Table 3.3) spans from Quaternary to the Lower Carboniferous, encountering the Cretaceous unconformity at 324 m MD over the Namurian, and the Dinantian at 992 m MD (i.e. the Goeree and Schouwen Members).

Table 3-3: Stratigraphy of the GVK-01 well (from www.nlog.nl)

Stratigraphical unit	Top interval	Base interval
QUATER. UNDIFF.	0	16
Breda Fm.	16	33
Rupel Fm.	33	85
Tongeren Fm.	85	125
Houthem Fm.	125	154
Ommelanden Fm.	154	324
Baarlo Fm.	324	672
Epen Fm.	672	926
Geverik Mb.	926	992
Goeree Mb.	992	1492
Schouwen Mb.	1492	1687

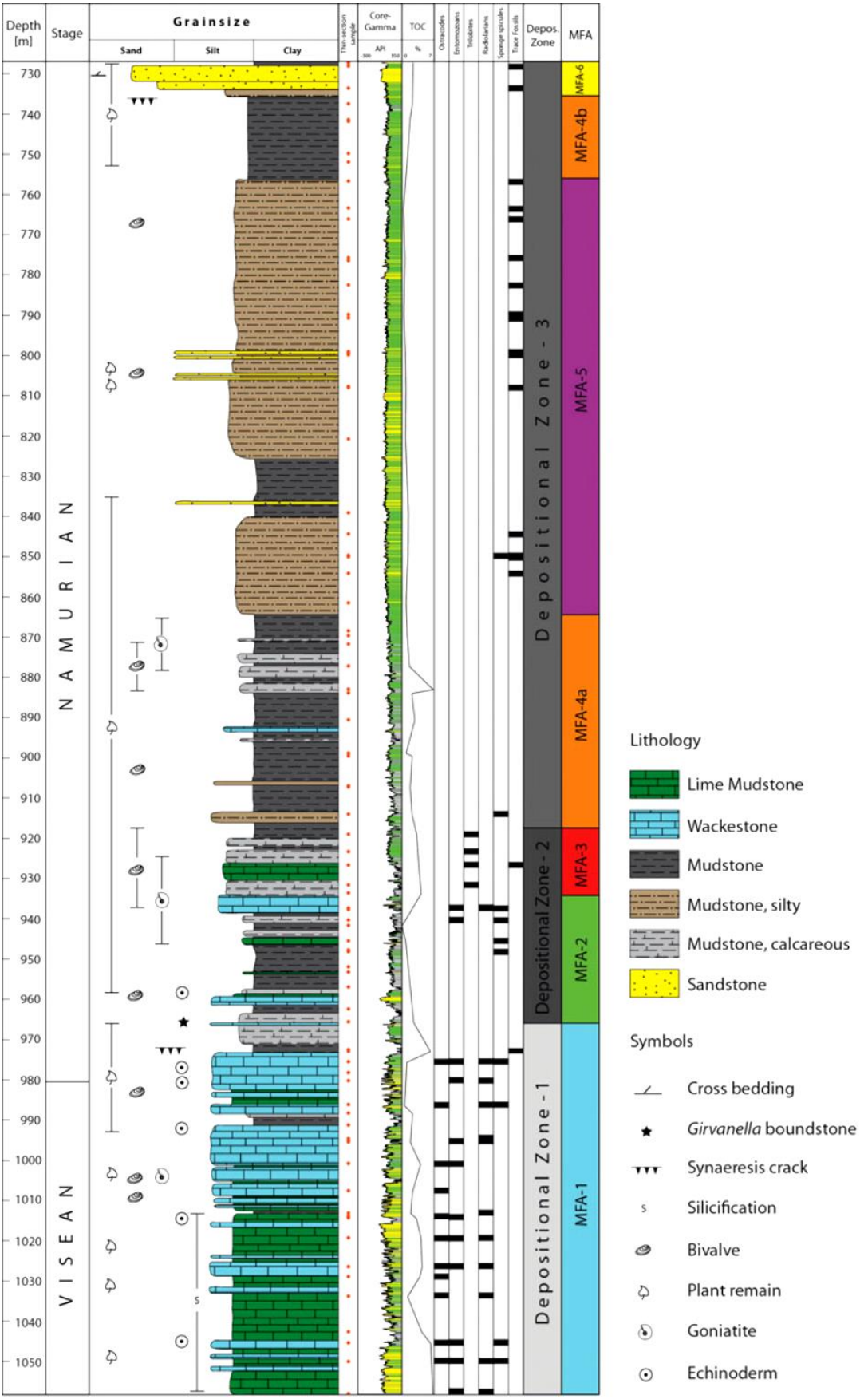

Figure 3-9: Cored interval in the GVK-01 well (interpretation by Nyhuis et al., 2016) (note that the Visean upper boundary is slightly higher than the top of the Zeeland Formation).

3.3.1 Dinantian interval

Four main microfacies types, in the Dinantian intervals encountered in the GVK-01 well, were recognised by Elf Aquitaine Production (1996):

1. "Autochtonous" grainstones enriched in algae and foraminifers,
2. Reworked and redeposited packstone-grainstones, with breccias, numerous lithoclasts and claystone intercalations with radiolarians (at the bottom), sponge spicules (at the top). Fragments of echinoids, bryozoa and brachiopods are fairly abundant, foraminifers are scarcer than in the previous microfacies,
3. Claystones,
4. Claystones with abundant to very abundant siliceous sponge spicules. Two radiolarian intervals (1575 and 1600 m) are identified and could be transgressive regional events.

The main paleoenvironmental evolution evolves from an inner platform setting, with algae and foraminifers, to an outer platform setting, with more and more reworked materials. The drowning of the platform goes on during the Upper Visean-Pendleian (?), with a thick interval of siliceous carbonate rocks devoid of autochthonous faunas.
A comprehensive microfacies analysis consist of 10 different types is described by Mathes-Schmidt (2000).

3.3.2 Depositional Environments

Elf Aquitaine Production (1996) described four sedimentary environments related to a complex storm-influenced carbonate ramp setting as following:

1. Offshore black shales,
2. "Lower ramp" deposits characterised by the presence of sponge spicules,
3. "Middle ramp" deposits bearing a large amount of crinoid debris,
4. "Upper ramp" deposits, characterised by the presence of oolites and bioclasts.

Accordingly, the Dinantian series draws a broad transgressive trend ending up at the transition with the Lower Namurian. The coarsest facies (packstone to grainstone) are organised in elementary fining-upwards strata, which are interpreted as storm deposits, although some gravity flow processes cannot be excluded. A secondary dolomitisation has destroyed the laminated structures that may have allowed to distinguish between the two processes. The textures vary from mudstone to packstone, with dolomite matrix dominant, minor intervals with calcite cement and some thin intervals showing strong silicifications.

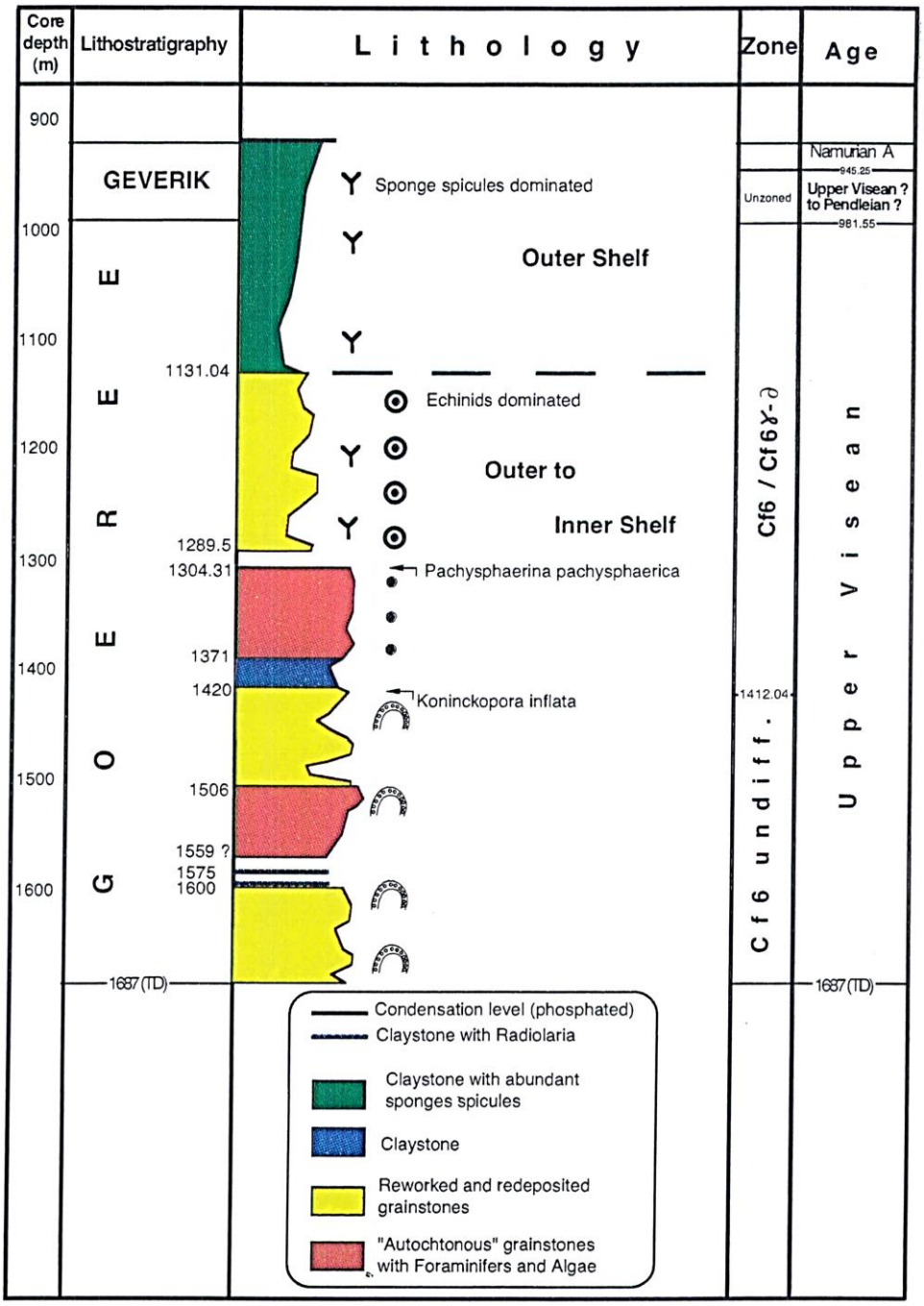

Figure 3-10: Environmental interpretation of the Dinantian succession as described by Elf Aquitaine Production (1996).

Mathes-Schmidt (2000) describes more in detail the evolution sedimentary successions in this well, but basically maintaining the same trend described by Elf Aquitaine Production (1996). The interval V3a to lower V3b is present in an open-marine, hemipelagic-shaped facies characterised by the alternation of quiet and higher-energy sedimentation phases on a carbonate ramp (facies association FA 1 of Mathes-Schmidt (2000). The sedimentation continues in V3b to shallow marine environments, with Palaeoberesellids benches in lagoonal environments, with bars and tidal channels (facies associations FA II-III).

These facies are replaced in the upper V3b/V3c first by proximal then distally turbiditic facies, and eventually turn into basinal facies with a partially cyclic structure (facies association FA IV). During the V3c a topographic flattening occurred and Porifera gained

increasingly in importance (facies association FA V). A later deepening during the transgression resulted in a sponge mud mound formation in a slope position (facies association FA VI). During upper V3c and Lower Namurian, the basin sedimentation switched to a clay-rich, relatively low-carbonate, basinal facies with spiculites forms (facies associations FA VII-IX). In the further lower Namurian, finally, the transition to a clay-silty, shallow-marine facies take place in relative proximity with a landmass (Facies Association FA X).

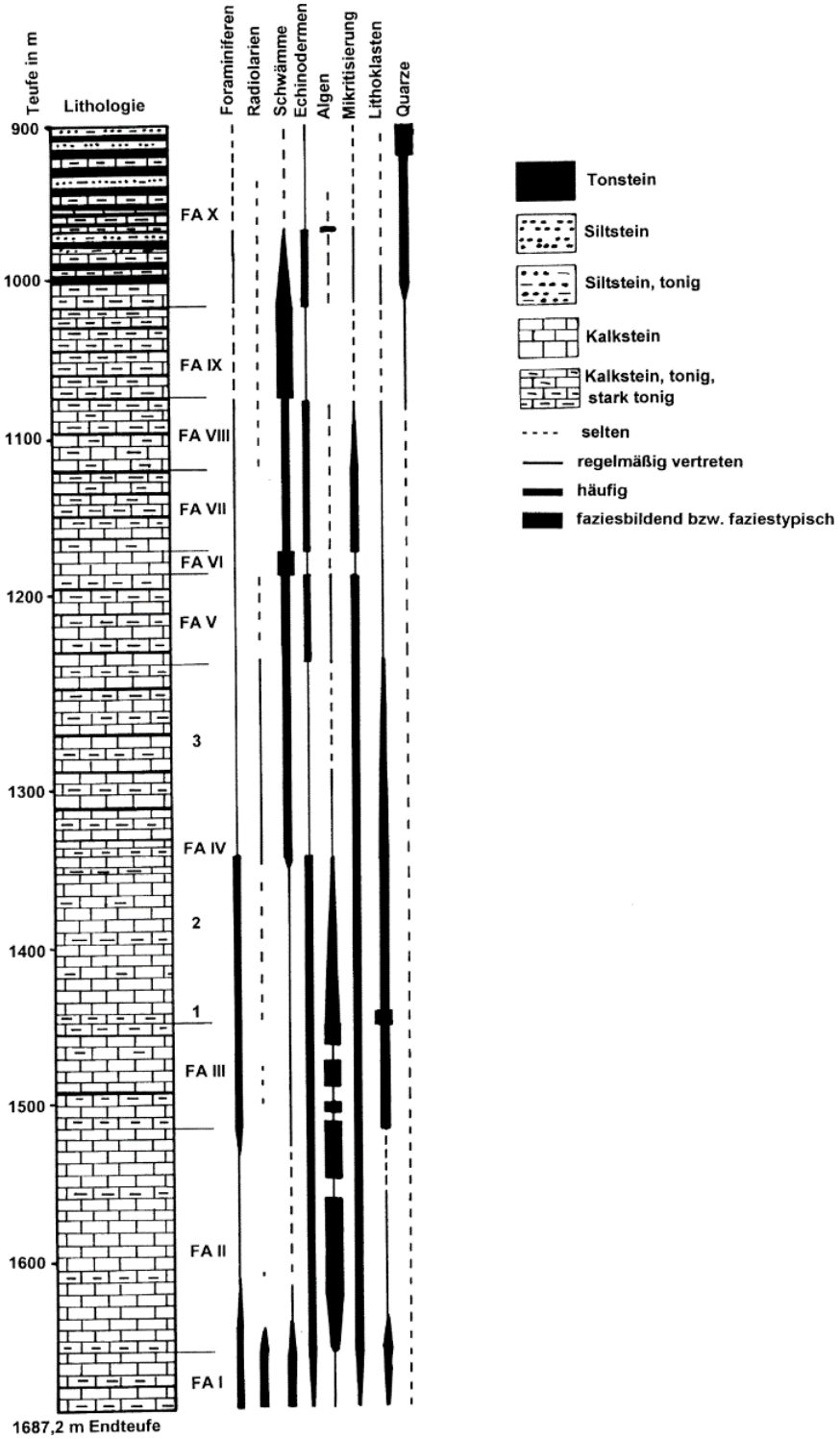

Figure 3-11: Facies evolution for the GVK-01 well (Mathes-Schmidt, 2000).

3.4 Biostratigraphy

The biostratigraphy of the GVK-01 intervals was analysed by Van de Laar (1987), Elf Aquitaine Production (1996), Mathes-Schmidt (2000) and Nyhuis et al. (2016). A comparison between Van de Laar (1987) and Mathes-Schmidt (2000) is shown in Figure 3-12. According to both authors, the Dinantian interval is entirely Visean, covering the V3a to V3c, Livian to Warnantian (Holkerian to Brigantian), with a major drowning during late Warnantian (Brigantian).

RGD Heerlen		Mathes Schmidt 2001	
Depth	Stratigraphy		Depth/Foraminifera, Conodonts
917,81 m			917,53 m
			942,20 m *Warnantella*
954,45 m	Nm	Nm	
			980,00 m
992,00 m		Nm? (Cf7?)	
	V3c	V3c	
1108,28 m			
1133,93 m			
	V3c		1226,00 m
1266,30 m		(Cf6δ)	
1279,00 m			
	V3bγ - V3c		1297,00 m
1305,12 m			
1306,53 m		V3c (Cf6δ)	1306,54 m *P. symmutatus, P. homopunctatus, G. bilineatus bilineatus, G. girtyi girtyi, G. girtyi intermedius*
	V3bγ-δ		1357,75 m *G. bilineatus bilineatus*
		- boundary V3b/V3c -	1334,00 m erster *Asteroarchaediscus*
1416,00 m		V3b	
1421,12 m			
		V3b	1460,60 m *Cribrospira panderi*
			1505,31 m *Paragnathodus homopunctatus*
		(Cf6γ)	1506,00 m *Howchinia*
	ob. V3bβ - V3bγ		1542,15 m *Koskinobigenerina*
1559,40 m			1545,55 m *Vissariotaxis*
		V3b	
1563,22 m		(Cf6β-γ)	
			1566,30 m *Cribrostomum*
	V3bα - V3bβ		
		V3a - V3b	1659,50 m bilam. Palaeotextulariidae
1669,18 m		(Cf6α-β)	
1672,09 m			
	V3a - V3bα		
1683,70 m			1687,20 m TD

Figure 3-12: Comparison between the biostratigraphy analysis reported by Van de Laar (1987) and Mathes-Schmidt (2000).

3.5 Sequence stratigraphy

In the current study (SCAN project), four depositional cycles, based on their gamma ray character, have been recognised in the Dinantian successions of the GVK-01 well (Table 3-4, Figure 3-13).

Table 3-4: Sequence stratigraphic scheme used on GVK-01 well.

Depositional cycles	**Gamma ray character**	**Depositional setting**
3b	Gamma ray increases upwards to very high followed by low gamma ray HST	Deposition in basin during LST and TST; high stand shedding of carbonates into basin. Carbonate system drowning during sequence 3b with increase of clastic input
3a		
2d	Generally high gamma ray	Distal carbonate ramp or basin
2c		

The overall depositional setting of the GVK-01 well is interpreted as basinal in which the carbonate intervals were introduced in the form of redeposited platform sediment. The depositional cycles are interpreted in terms of the evolution of surrounding carbonate platforms.

Cycle 2c: This cycle has a more uniform gamma ray signature and is interpreted as distal ramp or carbonate slope facies, possibly associated with a transition from carbonate ramp- to flat-topped carbonate platform. The low gamma ray intervals interpreted as influx of resedimented carbonates during high stands.

Cycles 2d to 3b: These cycles show an increasing-upward gamma ray signature that are interpreted as distal carbonate slope or basinal facies. The high gamma ray intervals are interpreted as LST to TST intervals when there was no carbonate production on platforms on exposed carbonate platforms and no export of peri-platform carbonates to the surrounding basin. The low gamma ray intervals are interpreted as HSTs when carbonate production was taking place on flooded carbonate platforms with some high stand shedding of carbonates to the basin.

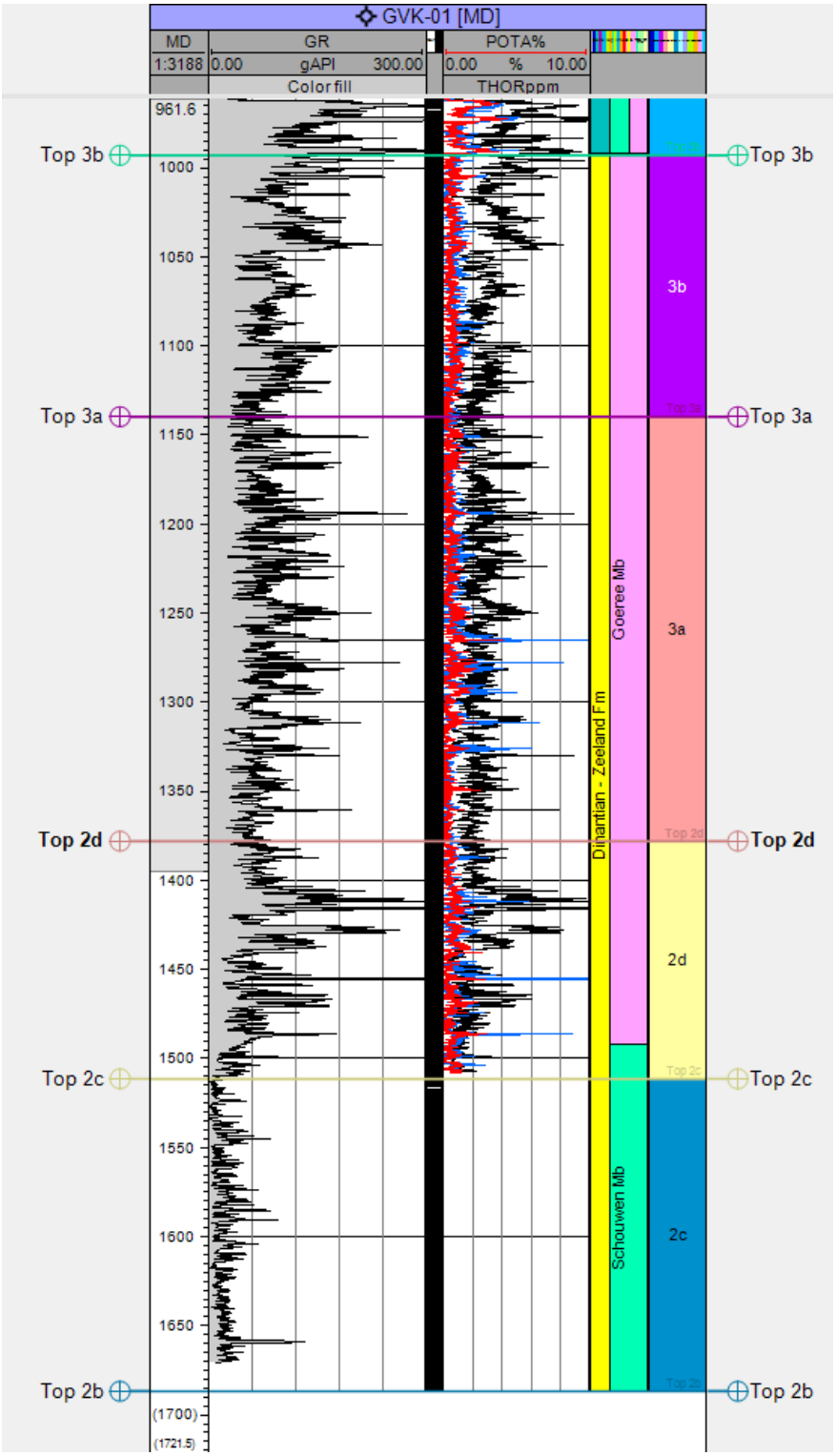

Figure 3-13: Depositional cycles and intervals distinguished in the GVK-01 well.

3.6 Facies

The cored GVK-01 well consists of dark shaly limestones (Figure 3-14) with scattered turbidites representing a basinal environment.

.

Figure 3-14: Cores 968.72-975 m (left) and 1038.87-1042.63 m (right) from the GVK-01 well.

3.7 Diagenesis

3.7.1 Paragenetic sequence

No thin sections were available to study the diagenetic phases of the GVK-01 core. The following description of diagenetic phases are retrieved from Mathes-Schmidt (2000). Accordingly, diagenesis of the GVK-01 carbonates commenced with micritisation, formation of a first cement (calcite A), syntaxial cement (SRZ), neomorphism and silcification. The diagenesis continued with the formation of blocky cements (B) and matrix replacive dolomites and incipient carbonate dissolution (Table 3-5). Dolomitisation, silicification and carbonate dissolution occurred during the burial diagenesis, therefore, the limits of early diagenesis is not clearly defined. Burial diagenesis is marked by carbonate dissolution, chemical compaction (stylolitisation), and weak coalification.

Table 3.5: Different diagenetic phases recognised by Mathes-Schmidt (2000).

Early diagenesis	Micritisation/microbial activity and micro-precipitation in FA VI/cement A/SRZ/physical compaction/neomorphosis/first silicification (? In radiolarian and spiculite)-chalcedony seams Blocky cements/recrystallisation/early carbonate solution (fitted fabric)/first idiomorphic dolomite crystals/further silicification
Burial diagenesis	progressive silicification and/or dolomitisation carbonate solution (solution sutures), incipient chemical compaction, dolomitisation (undulatory extinction) Coalification <4.0% Rmax Horizontal stylolites Brecciation/fracturing and filling

Microphotographs are not provided in the report by Mathes-Schmidt (2000). Consequently, it is difficult to link the diagenetic phases to the ones observed in KSL-02 and HEU-01 wells. A tentative correlation of the diagenetic phases of GVK-01 and HEU-01 and KSL-02 wells is presented in Figure 3-15.
Cement A and syntaxial calcite = C1
Matrix dolomite (MD) = D1 (The dolomite crystal habit is described as subhedral and no mention of saddle dolomite cement is made, therefore the dolomite is interpreted as an early matrix dolomite)
Blocky cement B = C2

HEU-01	KSL-02	GVK	Diagenetic phase
+	+	A?	C1
+	-	MD?	D1
+	+	B?	C2
+	+	+	Stylolites
+	+ (FI)	-	D2
+	+	-	C3
+	+	+	Si
+	+	-	Recrystallisation

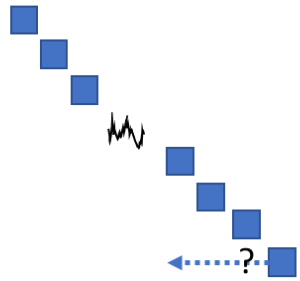

Figure 3-15: Overview of the diagenetic phases and their presence in the HEU-01 (S1), KSL-02 and GVK-01 wells. Note that there is also a minor early phase of silicification which is present in the GVK-01 well.

The fluid inclusion microthermometry data reported by Nyhuis (2012) were obtained mostly from quartz veins and rare calcite veins. The vast majority of the fluid inclusions are described as secondary in origin. The data does not allow differentiating the measurements from primary and secondary inclusions or the mineralogy of the host mineral, i.e. calcite or quartz. Plotting the data shows that two groups in the most likely secondary inclusions can be observed, i.e. a high (-35.5 °C <Tm ice< -28.5 °C) and a low salinity group (-6.4 <Tm ice< -0.9 °C). Inclusions of both groups are characterised by fairly high homogenisation temperatures (Figure 3-16) and the occurrence of CO_2 and CH_4 gas within the inclusions.
It could be speculated that the two fluid inclusion groups reflect fluid circulation triggered by two igneous events, i.e. the presence of CH_4 gas in the inclusions may point to an igneous source. The high salinity group may reflect fluid circulation associated with an igneous event during the early Permian when the Carboniferous rocks where deeply buried and potentially containing high salinity brines. The low salinity group may reflect a late Jurassic igneous event when the Carboniferous deposits where not buried to great depth and fresh water may have been circulating.

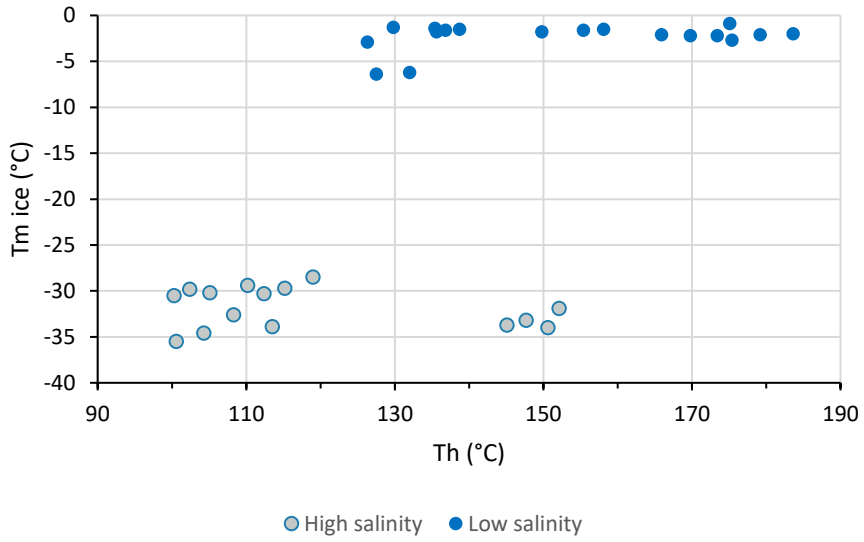

Figure 3-16: Cross plot of the fluid inclusion data reported by Nyhuis (2012). A high and a low salinity group can be observed in the data. The majority of the measurements were most likely obtained from secondary inclusions in quartz.

3.7.2 Diagenetic sequence in the context of burial/thermal history

A basic 1D basin model has been developed for this well, using as input the stratigraphy, the BHT data and the available vitrinite reflectance measurement, combined with the heat flow derived from Fattah and Verweij (2014), with a strong thermal event during Permian, related also to local intrusions. The model was developed in Petromod 2014.1 1D Express, developed by Schlumberger with the assumptions shown in Table 3-6. The heat flow model, temperature and burial curves are presented in Figures 3-17 to 3-20.

The computed erosion is about 4500 for the Permian unconformity and 1250 m for the Cretaceous unconformity.

Table 3-6: The input data for Petromod 1D.

Unit	Top	Btm	Erosion	Deposition		Erosion		Lithology
				From	To	From	To	
QUATER. UNDIFF.	0	16		2.5	0			Conglomerate (typical)
Breda Fm.	16	33		16	2.5			Sandstone (clay rich)
Rupel Fm.	33	85		32.5	28			Shale (typical)
Tongeren Fm.	85	125		35	32.5			Sandstone (arkose, typical)
Houthem Fm.	125	154		64.6	61.5			Sandstone (clay poor)
Ommelanden Fm.	154	324		94	66			Limestone (chalk, 75% calcite)
Missing Jurassic	324	324	250	200	150	150	137.5	Sandstone (clay rich)
Missing Triassic	324	324	500	251	200	137.5	125	Sandstone (clay rich)
Missing Permian	324	324	500	280	251	125	100	Sandstone (typical)
Missing Carboniferous	324	324	4500	318	300	294	280	Sandstone (typical)
Baarlo Fm.	324	672		321.82	318			Shale (organic lean, silty)
Epen Fm.	672	926		330.38	321.82			Shale (organic lean, silty)
Geverik Mb.	926	992		331	330.38			Shale (organic rich, typical)
Goeree Mb.	992	1492		335	331			Limestone (micrite)
Schouwen Mb.	1492	1687		343	335			Limestone (shaly)

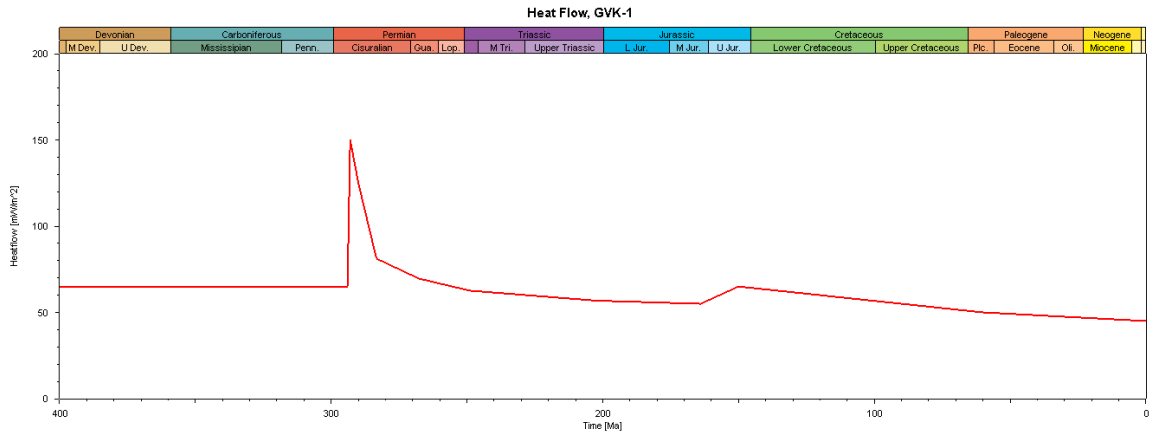

Figure 3-17: Heat flow model used, with a peak of 150 mW/m^2 during Early Permian.

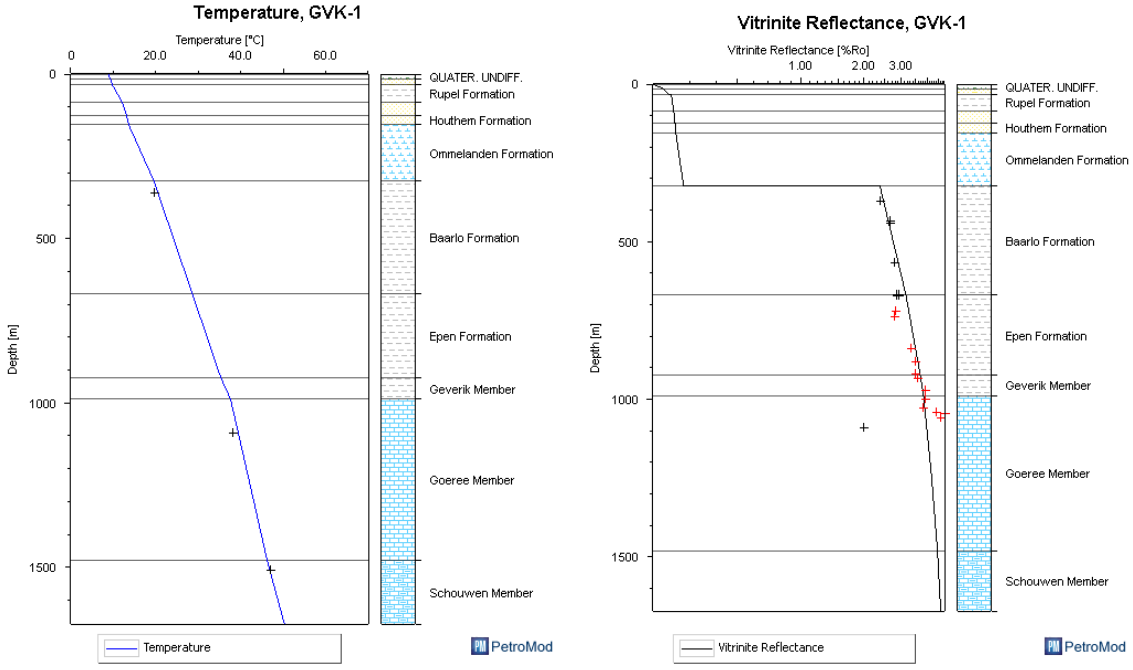

Figure 3-18: Temperature and maturity models and calibration points developed for the GVK-01 well.

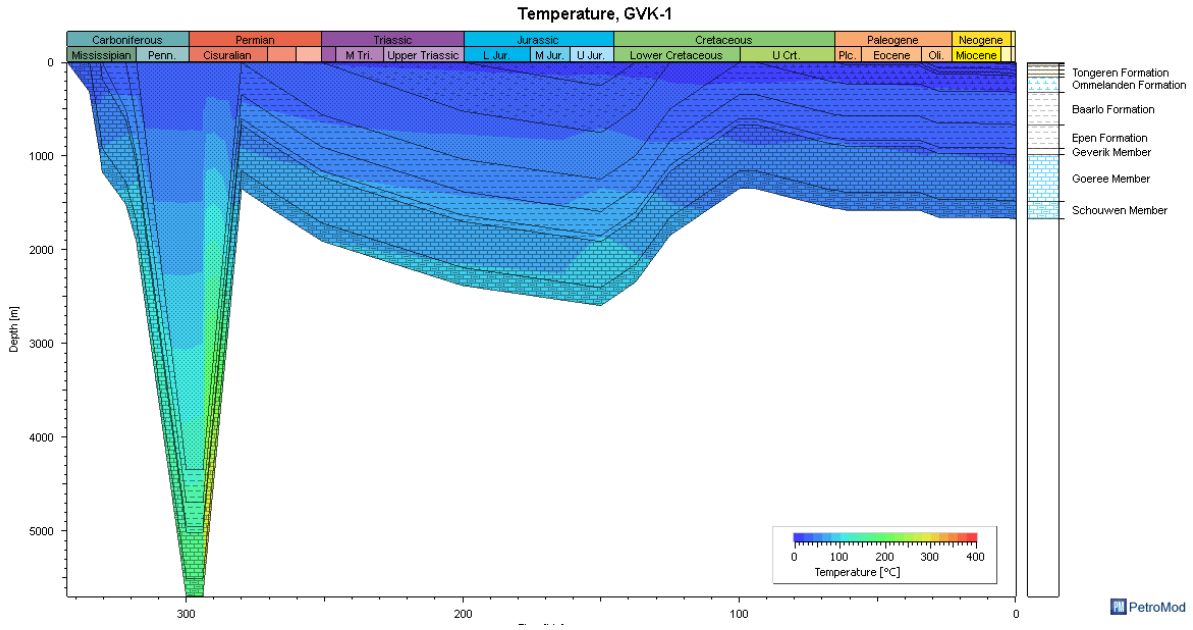

Figure 3-19: Burial curve and temperature model for the GVK-01 well.

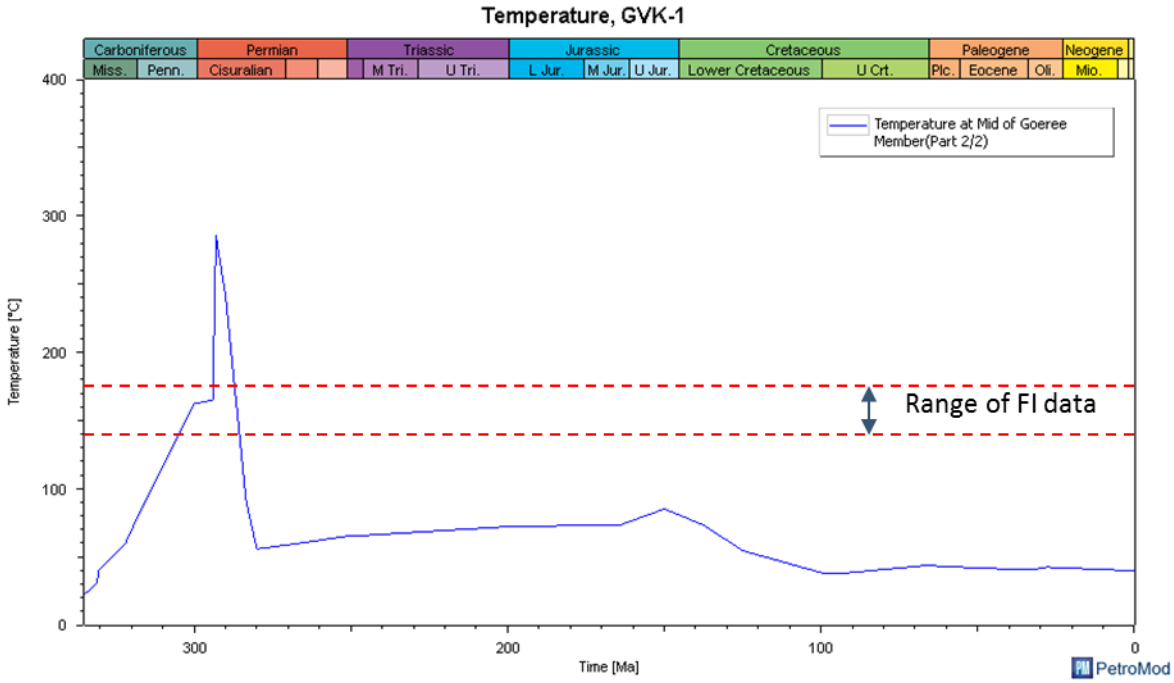

Figure 3-20: Modelled temperature for the Top Goeree Mb, compared with the available fluid inclusion data in the GVK-01 well.

3.8 Reservoir quality

Reservoir quality in the GVK-1 well is among the best for the Dinantian interval, with porosity values ranging from 0 to 10% (Figure 3-21). Core measurements are not available. Well tests revealed the presence of fracture porosity in the interval of 1125-1687 m (TNO, 2012).

This page intentionally left blank

Daalsesingel 1
3511 SV Utrecht
scan@ebn.nl
www.scanaardwarmte.nl

Onderzoek in de ondergrond voor aardwarmte